

## Chopping- and Funneling-Studies for ESS at Frankfurt

J. Madlung, A. Firjahn-Andersch, A. Schempp  
 Institut für Angewandte Physik, Johann Wolfgang Goethe-Universität  
 D-60054 Frankfurt/Main, Germany

### Abstract

The front end of the ESS linac has to provide a bunched high current beam with a special time structure for injection into the following DTL [1]. Therefore the layout contains beam funneling and chopping. A new concept for beam funneling using a two-beam RFQ and a multi-gap funneling deflector and first calculations for a new layout of the chopping line will be presented.

### 1. Introduction

The ESS reference design requires a 1.334 GeV H<sup>-</sup> linac beam optimized for injection into two compressor rings. The RFQ injector for the ESS linac provides a bunched beam of 107 mA at 5 MeV. This can be achieved by a system of two 175 MHz RFQ lines, each with a current of 54 mA, whose beams will be combined in a funnel section to a 107 mA beam with a bunch repetition rate of 350 MHz. For a proper operation of the compressor rings the linac beam must be chopped with a 60 % duty factor at the ring revolution frequency of 1.67 MHz which implies beam pulses of 360 ns and gaps of 240 ns during the macro pulse of 1.2 ms. The layout of the ESS linac is shown in figure 1.

In contrast to first funneling experiments with a system of discrete elements like quadrupole-doublets and -triplets, debunchers and deflectors [2,3,4], the first two-beam funneling experiment at the Institut für Angewandte Physik (IAP) in Frankfurt includes a two-beam RFQ where the beams are bunched and accelerated with a phase shift of 180° between each bunch. In the two-beam RFQ the beam separation is kept small. Therefore the rf-funneling deflector system can operate at low voltages.

A new concept, based on a resonator driven multi-gap deflector, where the ions are deflected several times, facilitates some constraints in beam funneling like the limitation of the electric field by rf-sparking. A combination of a two-beam-RFQ instead of the two single RFQs and such a multi-gap deflector could be used for the ESS linac.

Instead of earlier concepts with chopping in front of the first RFQ or even in the ion source the chopping of the ESS H<sup>-</sup> beam will be done between the two RFQ stages at an energy of 2 MeV. Here a clean chopping can be achieved due to the unneutralised, bunched beam. A travelling-wave electrostatic chopper, based on the BNL design, will be used to produce the time structure [5].

### 2. The two-beam RFQ for funneling

To study the properties of the new two-beam RFQ resonator, different kinds of prototype resonators were built and tested [6]. Also calculations with the MAFIA-code were done for comparison with the low-level measurements.

A prototype resonator with a reduced length and parallel beam axis has been designed and mounted into the 2 m long rectangular vacuum chamber. The resonator consists of two pairs of electrodes with a length of 100 cm supported by four symmetric stems in linear arrangement (Figure 2). Low-level measurements were done with the bead perturbation method. In high power tests the maximum rf-input power in pulsed mode was limited to 12 kW by the rf-power amplifier. At this power an electrode voltage of 27 kV was measured.

A 2 m long two-beam RFQ with convergent beam axes is under construction where the inner electrodes merge at the end of the structure. With this RFQ two single ion sources instead of a difficult two-hole extraction from one ion source can be used. While the parallel beam axes of the first prototypes would need a parallel beam shift in the funneling element, with convergent beam axes out of the new two-beam RFQ a shorter rf funneling deflector, placed before the beam crossing, is possible. Here the convergent beams will be bent to the new common axis.

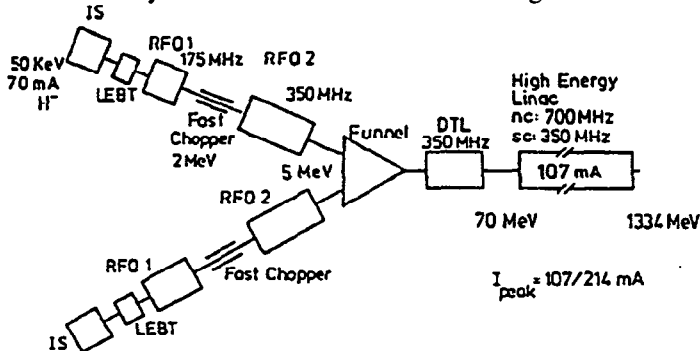


Fig. 1: Layout of the ESS linac.

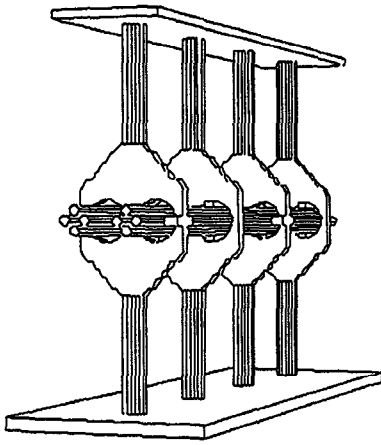


Fig. 2: MAFIA plot of the prototype two-beam RFQ structure.

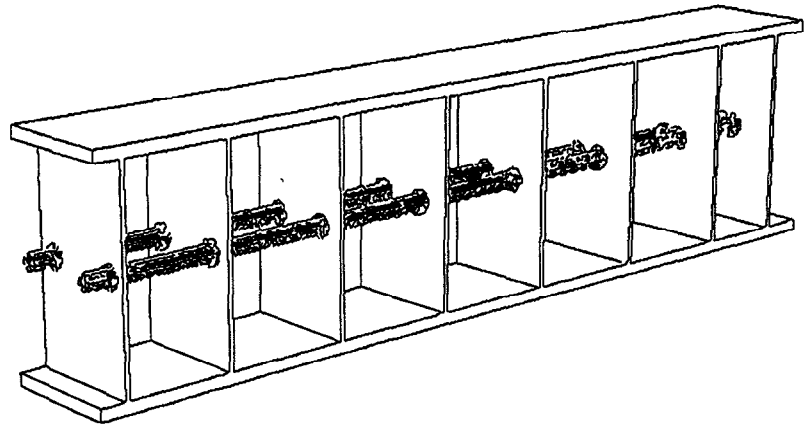


Fig. 3: MAFIA plot of the two-beam RFQ with convergent beam axes.

With an angle of 75 mrad between the beam axes the beam separation at the RFQ input will be more than 160 mm and 16 mm at the RFQ output. The electrodes are supported by eight flat stems. Figure 3 shows the resonator geometry as modelled by MAFIA. The RFQ electrode design with the use of the PARMTEQ code is in progress. For the phase shift of 180° between the bunches of each beam axis two different electrode designs with different electrode lengths are required.

### 3. The deflector geometry

The electrode geometry of the multi-gap deflector consists of some capacitors divided by spaces or sections with larger aperture with equal length. In this geometry the particles will see the deflecting field in one direction several times but the deflection in the opposite direction is always less. The length of the capacitors have to be proportional to the particle velocity and to the inverse of the frequency of the deflection system. The scheme of the multi-gap deflector electrode geometry and the behaviour of the particles along the deflector are shown in figure 4.

If the electric field is taken as a homogeneous and constant field over the cell length  $l$ , the single cells can be treated like separate rf-deflectors. For beam funneling the frequency of the deflector has to be the same as the accelerator frequency, so that the bunches from different beam axes will see opposite field directions, caused by the phase shift of 180° between each bunch. The advantage of the multi-gap deflector is a lower electric field than in single gaps. The field strength needed to bend a beam by 37.5 mrad is nearly 3 times less for a multi-gap deflector with 15 cells. Another option is to add focusing elements in the cells with larger aperture [7].

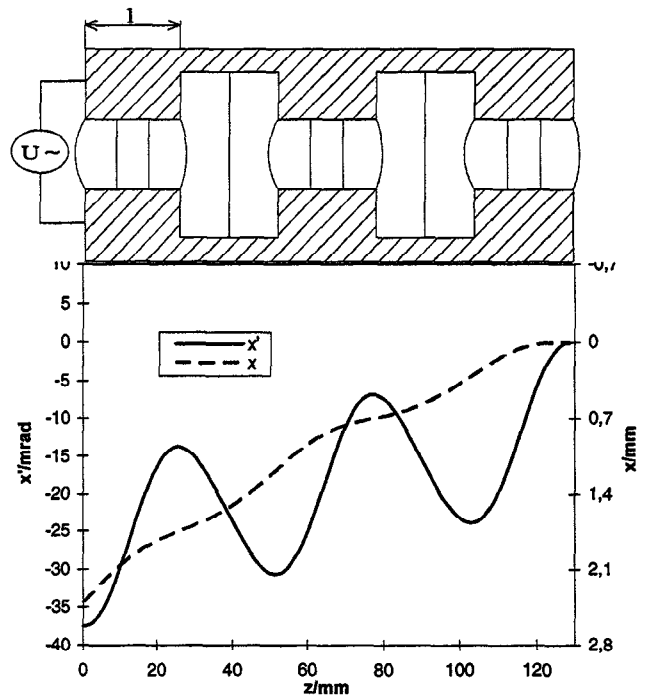


Fig. 4: Scheme of the multi-gap deflector electrode geometry and the behaviour of the deflection angle  $x'$  and the deflection  $x$ .

### 4. The funneling experiment

The funneling experiments will be carried out with  $\text{He}^+$ -ions to facilitate ion source operation and beam diagnostics. Two small multicusp ion-sources and electrostatic lenses, built by LBNL [8], will be used. The ion-sources and injection-lens will be attached directly on the front of the RFQ with an angle of 75 mrad. Behind the RFQ the funneling deflector will be placed before the beam crossing. Figure 5 shows the experimental setup of the funneling experiment. Beam diagnostics in front of and behind the RFQ and behind the funneling deflector are in preparation. The rf-resonator for the multi-gap deflector will be a structure as it is used for 4-Rod-RFQs with two stems. Each stem is electrically contacted with one of the deflector electrodes and will sustain the other electrode by a ceramic support. For longer electrodes it is possible to use an rf structure with more stems to preserve mechanical

stability. The resonator is under construction and a prototype for rf measurements has been finished. Figure 6a shows the output distribution of PARMTEQ calculations for the two-beam RFQ which are used as input for the particle simulations of the multi-gap deflector. In figure 6b the output is plotted. For an input distribution with displacement and angle in the opposite direction and a phase shift of  $180^\circ$  the results are the same. The bunch is bent  $37.5$  mrad to the common axis. These results show that such a system could be used for funneling. In table 1 the main parameters for the planned experiment with  $\text{He}^+$  and design parameters for the ESS funnel are listed.

two-beam RFQ	$\text{He}^+$	$\text{H}^+$
$f_0$ [MHz]	54	350
$T_{in}$ [keV]	4	2000
$T_{out}$ [MeV]	0.205	5
Length [m]	2	5.5/2.9
Angle between beam axes [mrad]	75	75
rf-deflector		
$f_0$ [MHz]	54	175
Voltage [kV]	9.5	230
Length [cm]	44	133
Length [ $\beta\lambda/2$ ]	15	15
Beam separation at input [mm]	16	50

Table 1: Main parameters of the planned experiment with  $\text{He}^+$  and design parameters for  $\text{H}^+$ .

### 5. Beam chopping

The chopping line between the two RFQs has to provide a good matching in both the transversal and the longitudinal plane for the unchopped beam as well as a total beam loss of the chopped beam. A first layout for an ESS chopping line by K. Bongardt [9] is shown in figure 7. The transversal focusing is achieved by quadrupole triplets where the chopper will be placed in the drift between the first two triplets and the beam stopper in the following drift section. Bunchers in front of and behind each triplet provide the longitudinal focusing.

An alternative layout is shown in figure 8. Here the chopper and the beam dump are placed in the same drift section.

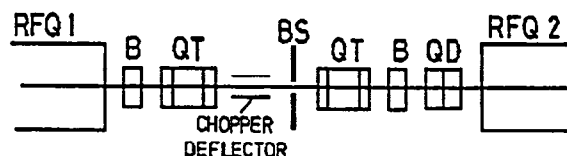


Fig. 8: Funneling line scheme by A. Schempp.

Beam dynamics calculations for this layout were done with the PARMTRA-code. In figure 9 the transversal behaviour of the beam along the funneling line is shown both for the unchopped (a) and chopped (b) beam. For these calculations a quadrupole doublet has been added to match the beam from the first RFQ to the triplet and a deflection force as high as  $100$  kV/m has been used.

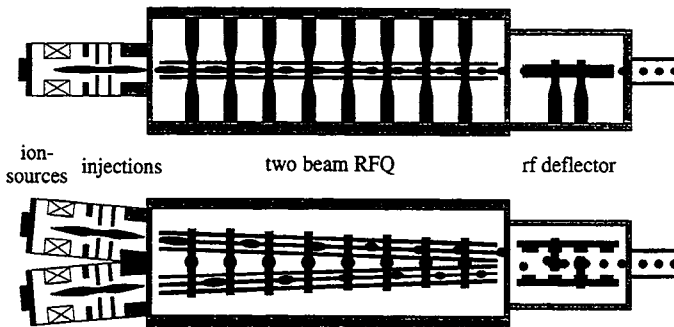


Fig. 5: Scheme of the planned experimental setup for funneling.

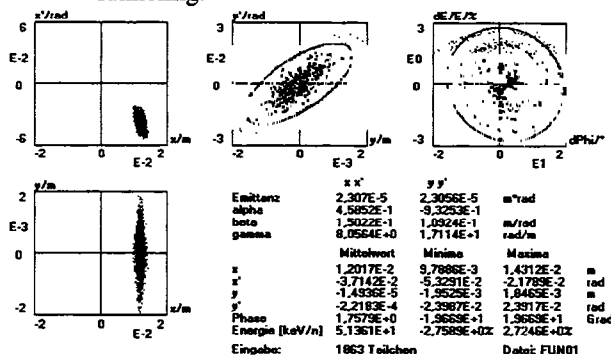


Fig. 6a: Input distribution for the funneling simulation.

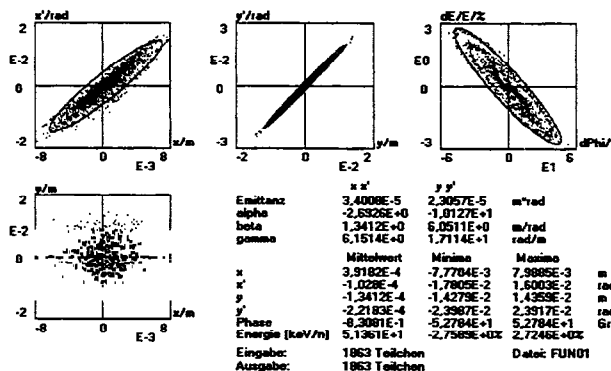


Fig. 6b: Output distribution of the funneling simulation.

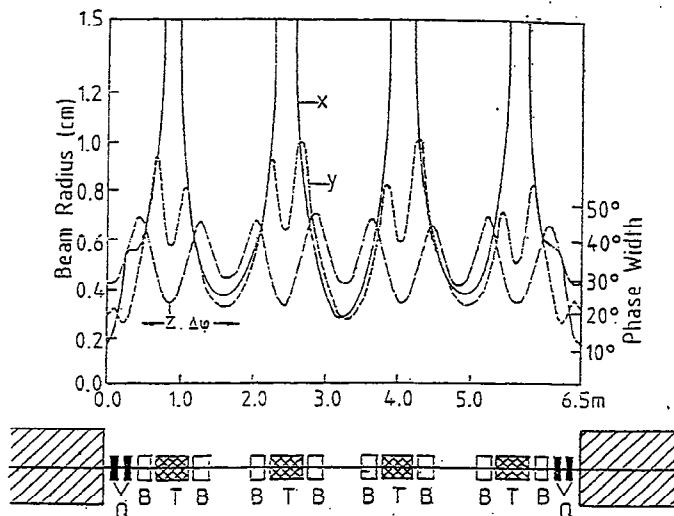


Fig. 7: Funneling line design by K. Bongardt.

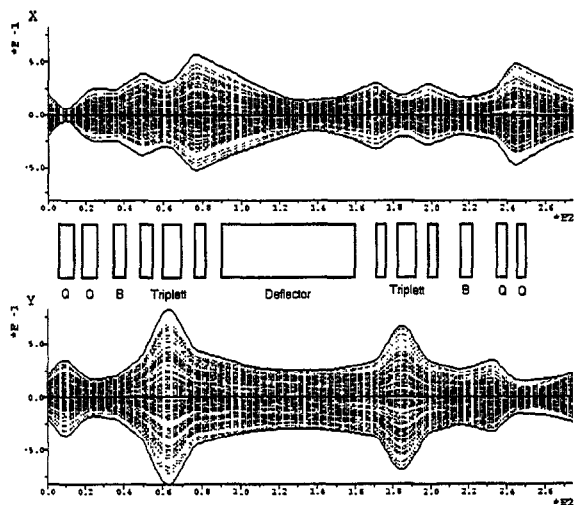


Fig. 9a: PARMTRA output of the chopping line simulation (chopper off).

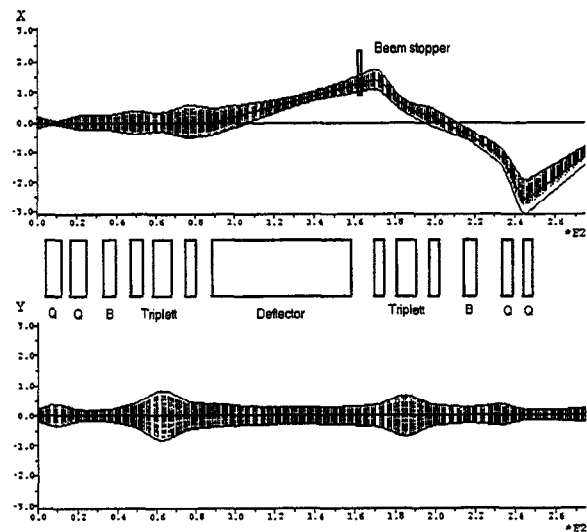


Fig. 9b: PARMTRA output of the chopping line simulation (chopper on).

For this layout the longitudinal focusing has to be investigated carefully. The beam power to be dumped is more than 2.5 kW, so that the beam dump has to be sufficiently cooled and probably more space has to be taken into account for the beam stopper.

The chopper will be a pulsed electrostatic deflector with deflection plates segmented into strips transversal to the beam direction. They are connected by coaxial delay lines, so that the pulse velocity along the beam direction is matched to the beam velocity. One set of strips above and below the beam will halve the magnitude of the voltage needed for deflection. In figure 10 a schematic drawing of the chopper is shown. For the ESS case the rise and fall time of the chopping voltage has to be less than 4.5 ns to reach a clean chopping.

## 6. References

- [1] Outline Design of the European Spallation Neutron Source, Editors: I.S.K. Gardner, H. Lengeler, G.H. Rees, ESS/P1/95
- [2] K. Bongardt and D. Sanitz, Funneling of Heavy Ion Beams, Primary Report, Kernforschungszentrum Karlsruhe, 11 04 02P14C (1982)
- [3] J.F. Stovall, F.W. Guy, R.H. Stokes and T.P. Wangler, Beam Funneling Studies at Los Alamos, Nucl. Instr. and Meth. A278 (1989) 143
- [4] K.F. Johnson, et al., A Beam Funneling Demonstration: Experiment and Simulation, Part. Acc. Vols. 37-38 (1992) 261-268
- [5] J.M. Brennan, et al., A Fast Chopper for Programmed Population of the Longitudinal Phase Space of the AGS, BNL-41832, PAC89, IEEE CH2669 (1989) 1154
- [6] A. Firjahn-Andersch, A. Schempp, C. Staschok, J. Madlung, A Two-Beam RFQ for Funneling of Ion Beams at Low Energies, GSI-Report, GSI-95-06 (1995) 25
- [7] A. Schempp, Beiträge zur Entwicklung der Radiofrequenzquadrupol-(RFQ)-Ionenbeschleuniger, Habilitationsschrift, Universität Frankfurt am Main (1990)
- [8] K.N. Leung, Multicusp Ion Sources, Proc. 5th Int. Conf. Ion Sources, Beijing, China (1993) 1165-1169
- [9] K. Bongardt, Matching Problems between Linac and Compressor Ring, ESS-Report 94-8-L (1994)

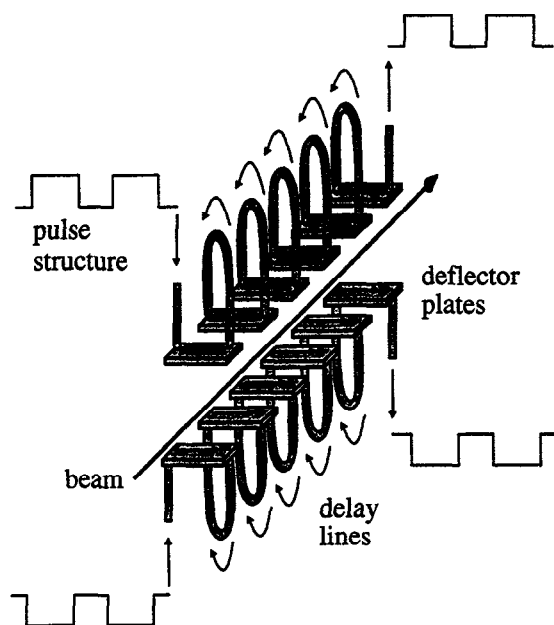


Fig. 10: Schematic drawing of the chopper.